Upper-Air Data Validation and Analysis

- Introduction
  - Terminology
  - Upper-Air Instruments
- Other Sources of Upper-air Data
- Terminology
- Upper-Air Instruments
- Upper-Air Data Validation
- Common Problems Encountered in Upper-Air Meteorological Data
- Interpreting Upper-Air Meteorological Data Displays
- Example Upper-Air Data Validation

- Investigating Upper-Air Meteorological Data
- Radar Profiler Reflectivity C_n^2
- Investigating Boundary Layer Structure and Evolution
- Isentropic Analysis
- Trajectory Analyses
- Ventilation and Recirculation Analysis
- Available Methods and Tools
- Summary
- References

Introduction

- The PAMS program requires one upper-air meteorological measurement station per PAMS network with four soundings per day of winds and temperature.

- These measures of upper-air meteorology are critically important to several PAMS analyses including:

  - Investigating the boundary layer structure and evolution including the spatial and temporal characteristics of mixing height.

  - Investigating ozone and precursor transport.

- Instruments that provide these measurements are rawinsondes, radar wind profilers with radio acoustic sounding systems (RASS), and SOund Detection and Ranging (SODAR) systems with RASS.

- Radar wind profilers with RASS provide hourly averaged vertical profiles of winds, virtual temperature, and related quantities such as the radar reflectivity structure parameter, which can be used to estimate mixing depth.

Other Sources of Upper-Air Data

Other sources of upper-air meteorological and air quality data include these non-PAMS sources:

- Aircraft instrumented to measure ozone, nitrogen oxides, hydrocarbons, carbonyl compounds, SO_2, CO, meteorological observables, position, and altitude.

- Satellite photographs.

- Tethersondes and ozonesondes measurements of ozone concentrations as a function of altitude.

- Light detection and ranging (Lidar - absorption of light by molecules) ozone measurements as a function of altitude.

Terminology

- In this section, we have used the terms "depth of the mixed layer", "mixing height", and "mixing depth" synonymously.

- Mixing height is defined as the height above the surface through which relatively vigorous mixing will take place due to convection. Mixing heights commonly go through large diurnal variations and seasonal variations.

- Another way to define the mixing height is the distance between the ground and the inversion base. The location of the inversion base will be dependent on the weather conditions that produce the inversion. Usually it's sinking air aloft, or subsidence, with stronger subsidence producing lower inversion bases (and hence higher pollution concentrations). Thus, pollution released at the ground can mix upward until it reaches the inversion base, and then its upward mixing is strongly inhibited. If the inversion base is close to the ground, then the pollution is confined to a small volume of air next to the ground, resulting in high pollution concentrations.

Upper-Air Instruments

System	Variables[a]	Approx. Frequency	Height Range (km)	Resolution (m)
Rawinsonde	WS, WD, T, RH, Td, p mixing height	404 MHz 1680 MHz	3 to 5	p, T, T_d, RH: 5-10 Winds: 45-75
Mini-SODAR	WS, WD, u, v, w,	3-5 kHz	<0.3	5 - 20
Standard SODAR	WS, WD, u, v, w, turbulence, mixing height	1-3 kHz	<2	20 - 50
Mega-SODAR	WS, WD, u, v, w, turbulence, mixing height	<1 kHz	<5	100 - 200
Radar profiler	WS, WD, u, v, w, mixing height	915 MHz	<5	60 - 200
RASS	T_v	2 kHz	<2	60 - 200

[a] Where WS = wind speed; WD = wind direction; u, v, and w are the east-west, north-south, and vertical components of the wind, respectively; T = dry bulb air temperature; T_d = dew point temperature; T_v = virtual temperature; RH = relative humidity; and p = pressure. (U.S. EPA, 1995)

Upper-Air Data Validation

- As with surface air quality and meteorology, in order to ensure valid data analyses, the validity of the data needs to be assessed. Several screening tests should be performed on the upper-air data including automated and manual checks before the data are used.

- Automated data screening tests for upper-air meteorological measurements include temporal and vertical consistency checks such as:

  – Wind shear checks - *Look for large changes that may not be real.*

  – Hydrostatic checks (temperature) - *Look for large changes that may not be real.*

Upper-Air Data Validation

- Manual data screening tests for upper-air meteorological measurements include:

  - Meteorological reasonableness checks with climatology and local and regional weather conditions - *Do significant changes in wind or temperature data make physical sense with respect to changes in weather conditions?*

  - Vertical and temporal consistency checks for continuous (hourly) data include comparing adjacent times, heights, and sites. *For example, do changes from hour to hour, from altitude bin to altitude bin, or from site to site make physical sense?*

- It is important to include the following in an upper-air data validation process:

  - Establish dominant (prevailing) weather pattern (i.e., using synoptic weather maps) and changes in weather due to the passage of a cold front, for example.

  - Examine each individual profile.

  - Attempt to identify the cause of outliers (i.e., meteorological phenomena or instrument problem?)

  - Use other supporting data (e.g., surface meteorology and air quality, weather maps, satellite photographs, reflectivity, etc.) to confirm outliers or large changes with time or location.

Common Problems Encountered in Upper-Air Meteorological Data (1 of 4)

For Rawinsonde systems, the following are potential problems:

- Poor ventilation may occur if the instrument's air channels become obstructed during operation or due to a manufacturing defect. *This may result in unrepresentative readings of temperature (T) and relative humidity (RH) (and thus dew point temperature) at or near the surface.*

- Radio frequency (RF) interference *may occasionally produce erroneous T, dew-point T, and RH measurements, which appear as spikes in the data when plotted in a time series or profile plot.*

- Uncertainties in the position tracking mechanism can be caused by factors such as RF interference, downbursts or updrafts, or icing conditions. *This may result in unrealistic changes in the wind speed and direction, especially when the antenna's elevation angle is less than about 10 degrees.*

- Icing can occur when a balloon encounters clouds and precipitation zones where the T is below freezing causing the balloon to descend. Once the balloon descends below the freezing level, the ice melts and the balloon re-ascends. *This causes unrepresentative wind and thermodynamic data.*

US EPA (2000)

For SODAR wind profiler systems, the following are potential problems:

- Fixed echo reflections or "ground clutter" occurs when nearby obstacles reflect the sodar's transmitted pulse. *Depending upon atmospheric conditions, wind speed, background noise, and signal processing techniques, the fixed echoes may reduce the velocity measured along a beam(s) or result in a velocity of zero.*

- Ambient noise interference can come from road traffic, fans or air conditioners, animals, insects, strong winds, etc. *Loud broad-spectrum noise will decrease the signal-to-noise ratio (SNR) of the sodar and decrease the performance of the system.*

- Reduced altitude coverage due to debris in the antenna.

- Precipitation interference. *During rainfall events, the sodar may measure the fall speed of drops which will produce unrealistic winds. Also, the sound of the droplets hitting the antenna can increase the ambient noise levels and reduce the altitude coverage.*

US EPA (2000)

For radar wind profiler systems, the following are potential problems:

- Interference from migrating birds. Birds act as large radar targets so that signals from birds overwhelm the weaker atmospheric signals. *This can produce biases in the wind speed and direction measurements.*

- Precipitation interference. During precipitation, the profiler measures the fall speed of rain drops or snowflakes.

- Ground clutter occurs when a transmitted signal is reflected off an object such as trees, power lines, or buildings instead of the atmosphere. *Data contaminated by ground clutter can be detected as a wind shift or a decrease in wind speed at affected altitudes.*

- Velocity folding or aliasing occurs when the magnitude of the radial component of the true air velocity exceeds the maximum velocity that the instrument is capable of measuring. *Folding occurs during very strong winds (>20 m/s) and can be identified and flagged by automatic screening checks.*
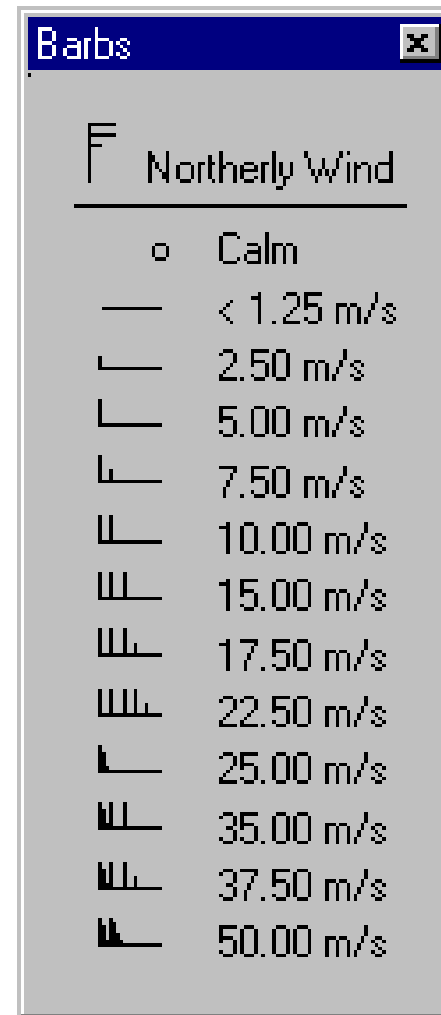
For RASS systems, the following are potential problems:

- Vertical velocity correction. Vertical motions can affect the RASS virtual T measurements. Virtual T is determined by measuring the vertical speed of an upward-propagating sound pulse, which is a combination of the acoustic velocity and the atmospheric vertical velocity. *If the atmospheric vertical velocity is non-zero and no correction is made for the vertical motion, it will bias the T measurement.*

- Potential cold bias. *Under certain conditions (possibly associated with site selection issues), RASS observations may exhibit a bias of -1°C or so.*
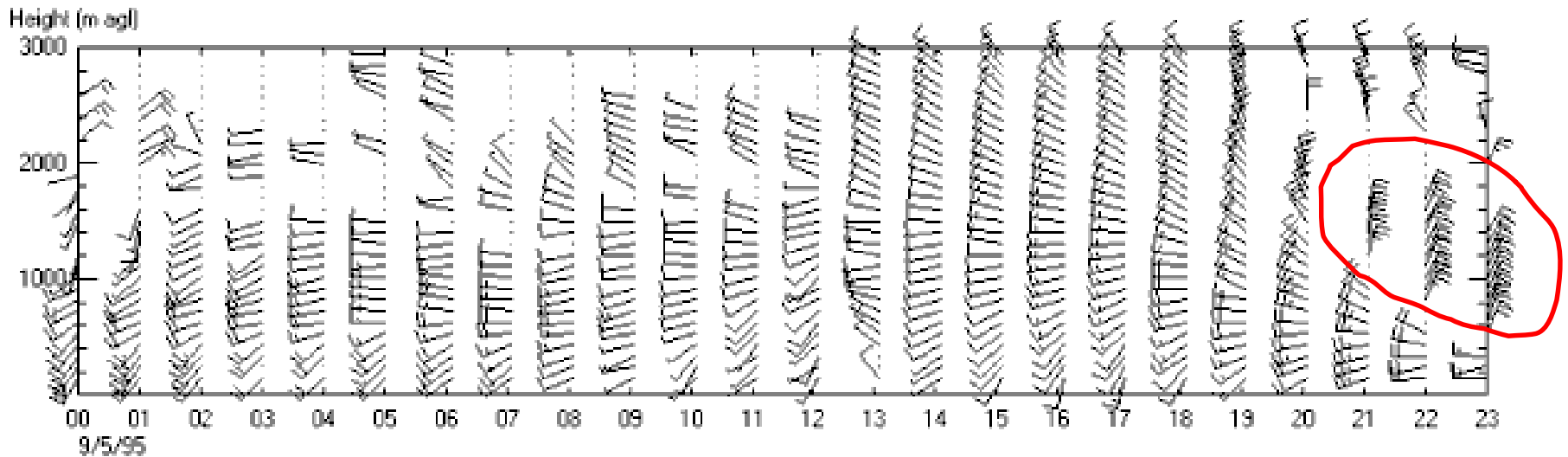
Interpreting Upper-Air Meteorological Data Displays

- This figure shows an example key to the wind barbs shown in several figures in this section of the workbook.

- The number, size, and often color of tick marks on the bar represent different wind speeds.

- The orientation of the barb indicates wind direction (i.e, barb or flag up = wind from the north).


| Barbs	
	Northerly Wind
o	Calm
	< 1.25 m/s
	2.50 m/s
	5.00 m/s
	7.50 m/s
	10.00 m/s
	15.00 m/s
	17.50 m/s
	22.50 m/s
	25.00 m/s
	35.00 m/s
	37.50 m/s
	50.00 m/s

- This example of bird contamination in radar profiler data shows a time-series plot of wind speed and direction at various altitudes for a 24-hour period. The orientation of the barb indicates wind direction (barb or flag up = wind from north). A larger number of tails on the barbs indicates increasing wind strength.

- The northerly winds from 2100 and 2300 EST between 500 and 2000 m above ground level (agl) were actually caused by the radar measuring the motion of birds migrating to the south, instead of the northwesterly atmospheric winds. Birds act as large radar "targets," so that signals from birds overwhelm the weaker atmospheric signals.

- Birds generally migrate year-round along preferred flyways, with the peak migrations occurring at night during the Spring and Fall months (Gauthreaux, 1991). Additional information about bird contamination of radar wind profiler data can be found in Wilczak et al. (1995).
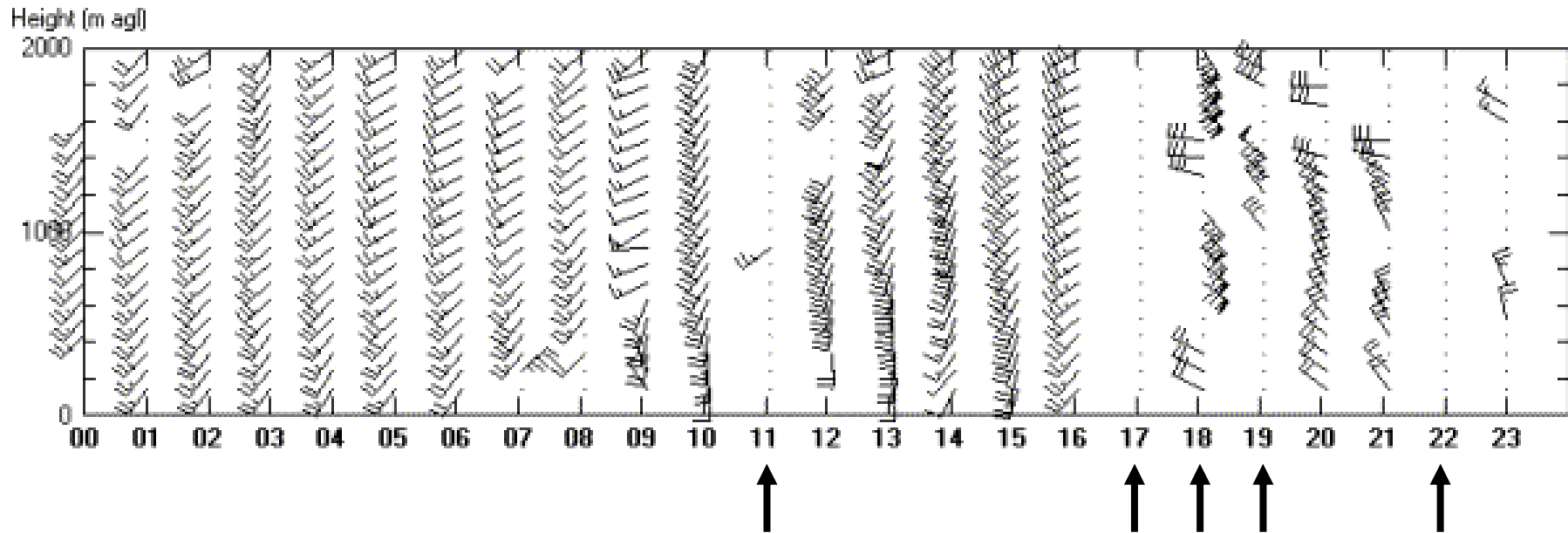
- Another type of natural phenomenon that can invalidate upper-air meteorological data is precipitation. This example shows precipitation interference in radar profiler data. Missing wind data at 1100, 1700-1900, and 2200 EST were caused by precipitation.

- During precipitation, the radar profiler measures the fall speed of rain drops or snow flakes. In this example, the profiler measured strong, downward motion of -3 to -8 m/s (observable in the raw data), which is actually the motion of the rain drops. Missing winds resulted when the radar measured both atmospheric and precipitation motions and the sub-hourly data failed quality control checks (Dye, 1996).
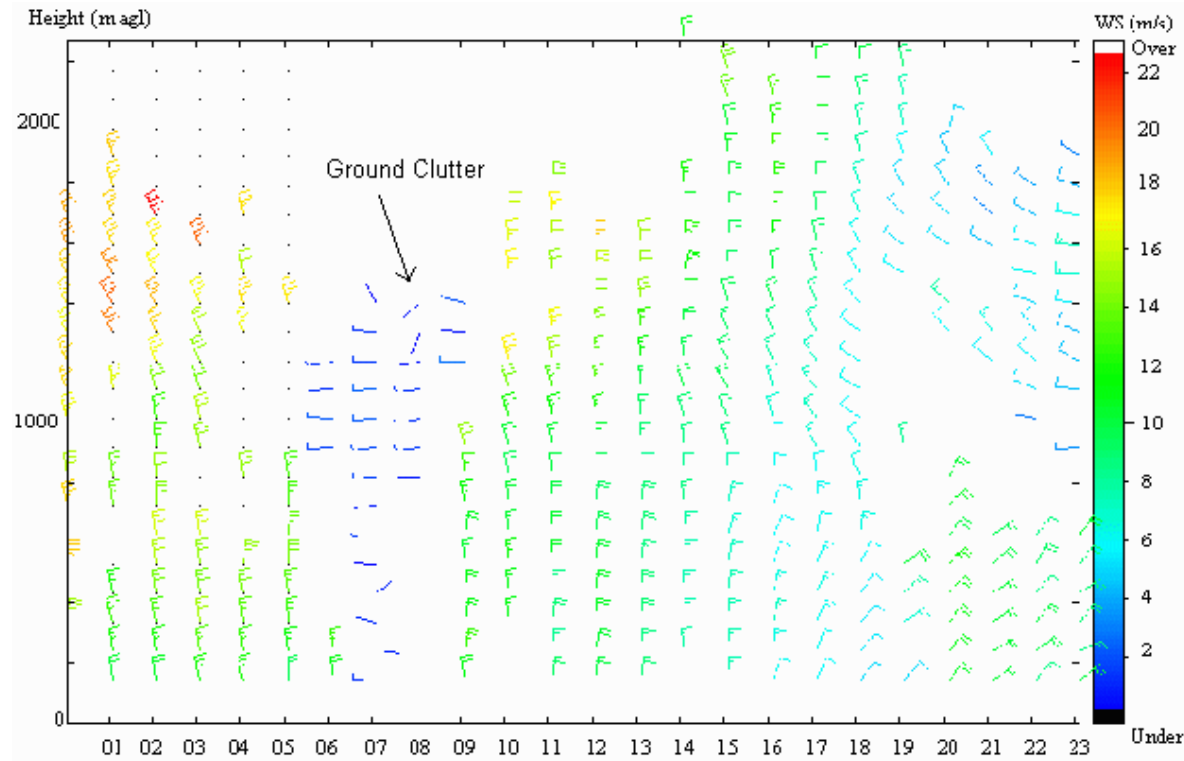
- Recurrent and excessive ground clutter can seriously damage data quality. Siting issues are very important. This figure shows an example of ground clutter interference from a radar profiler site. Ground clutter is caused when a transmitted signal is reflected off an object instead of the atmosphere. In this case, the radar signals were reflected off distant trees, which produced the light winds between 0600 and 0800 EST (Dye, 1996).

Investigating Upper-Air Meteorological Data

- Estimate mixing heights from radar profiler reflectivity (C_n^2) and RASS data and prepare diurnal plots of mixing heights.

  The depth of the mixed layer is a critical parameter for understanding the formation, dispersion, and transport of ozone and precursors during pollution episodes.

- Compare mixing height estimates made from various measurement techniques.

- Investigate temporal (day-to-day), spatial, and episode versus non-episode differences in mixing heights.

- Prepare time-height cross sections of winds and potential temperature at selected locations (e.g., important locations where sufficient data are available).

- C_n^2 is a measure of the variations in the refractive index of the atmosphere. Turbulence produces variations in atmospheric temperature, humidity, and pressure, which in turn cause variations in the radio refractive index.

- C_n^2 is a useful parameter for estimating daytime mixing depth and nighttime residual layer structure.

- The reference list provides equations for computing C_n^2 and guidance in its use.

Radar Profiler Reflectivity C_n^2 (2 of 2)

- Theory: C_n^2 is largest at the inversion which caps the convective boundary layer (Wyngaard and LeMone, 1980).

- Observations:

    - Mixing depth equals the peak in the C_n^2 profile.

    - C_n^2-predicted mixing depth has been verified against rawinsonde data (White, 1993) and aircraft data (Dye et al., 1995a).

- C_n^2 is useful to:

    - Determine the maximum mixing depth

    - Diagnose the growth of the mixed layer

    - Compare with model estimates

- It is important to compare estimates of mixing depth made using different methods. This example shows a scatter plot of C_n^2 -derived mixing depths and mixing depths estimated from aircraft profiles of pollutant concentrations, turbulence, and temperature.

- The agreement is quite good, except for one outlier, which can be explained by the difficulty in identifying a mixing depth when several pollutant layers are observed.
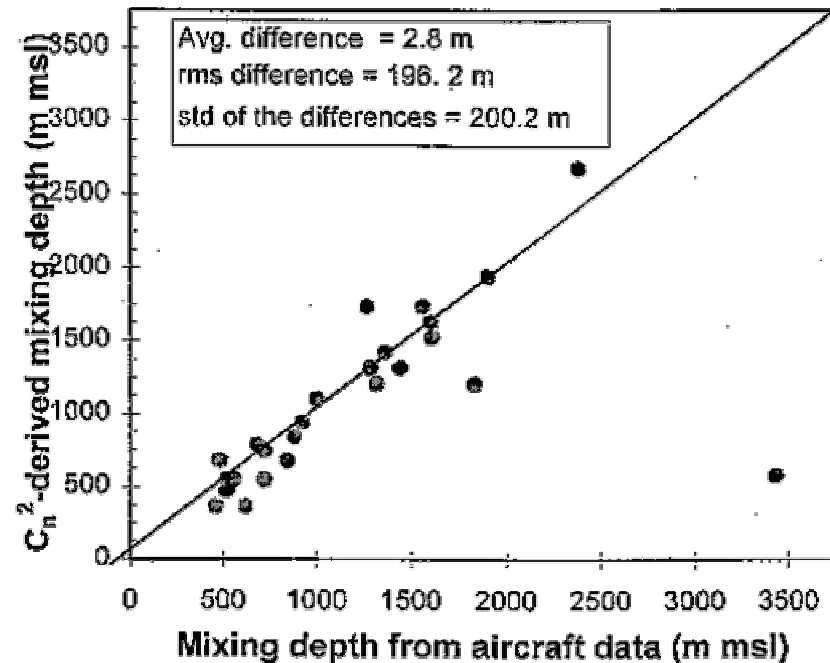

Twenty-five comparisons were made using aircraft data collected in the afternoon near three profilers deployed in southeast Texas (SAI et al., 1995). Mixing depth is provided in meters above mean sea level (m msl). The average difference between the measurement types was about 3 m; the root mean square (rms) difference was about 200 m; and the standard deviation (std) of the differences was 200 m.

- This example also compares C_n^2 profile from a radar profiler with profiles of turbulence, ozone concentration, and temperature measured by an aircraft during a descent over the site.

- The C_n^2 profile peaks at 800 and 2400 m, which corresponds to the tops of two polluted layers. The first layer, from the surface to 800 m, was well mixed as indicated by high, uniform ozone concentrations and strong turbulence. This layer was capped by a weak stable layer between 800 and 1000 m, and the peak value of C_n^2 closely corresponds to the top of this mixed layer.

- The ozone and turbulence data suggest that mixing had occurred in the layer from 800 to 2300 m; the pollutants in this layer were likely vented by updrafts and clouds ahead of a sea-breeze front.
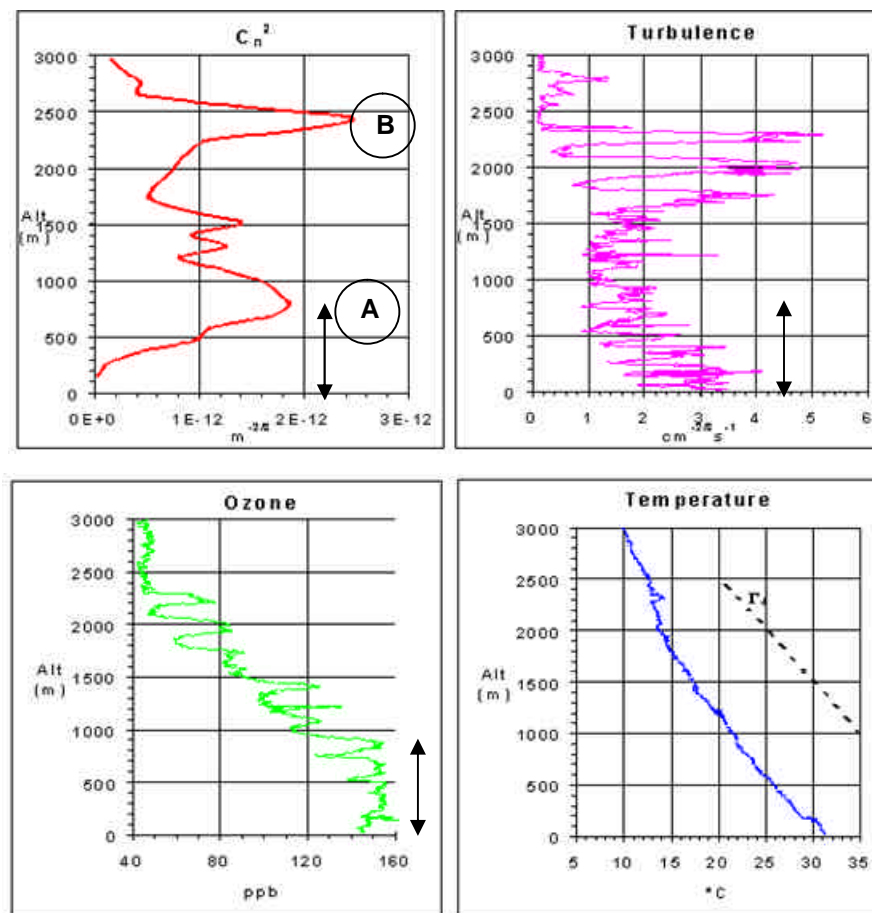
An understanding of mixing depth and other upper-air parameters enhances air quality analysis. This figure reveals two inversion layers corresponding to the C_n^2 maxima (A and B in top left) (Dye, 1996).
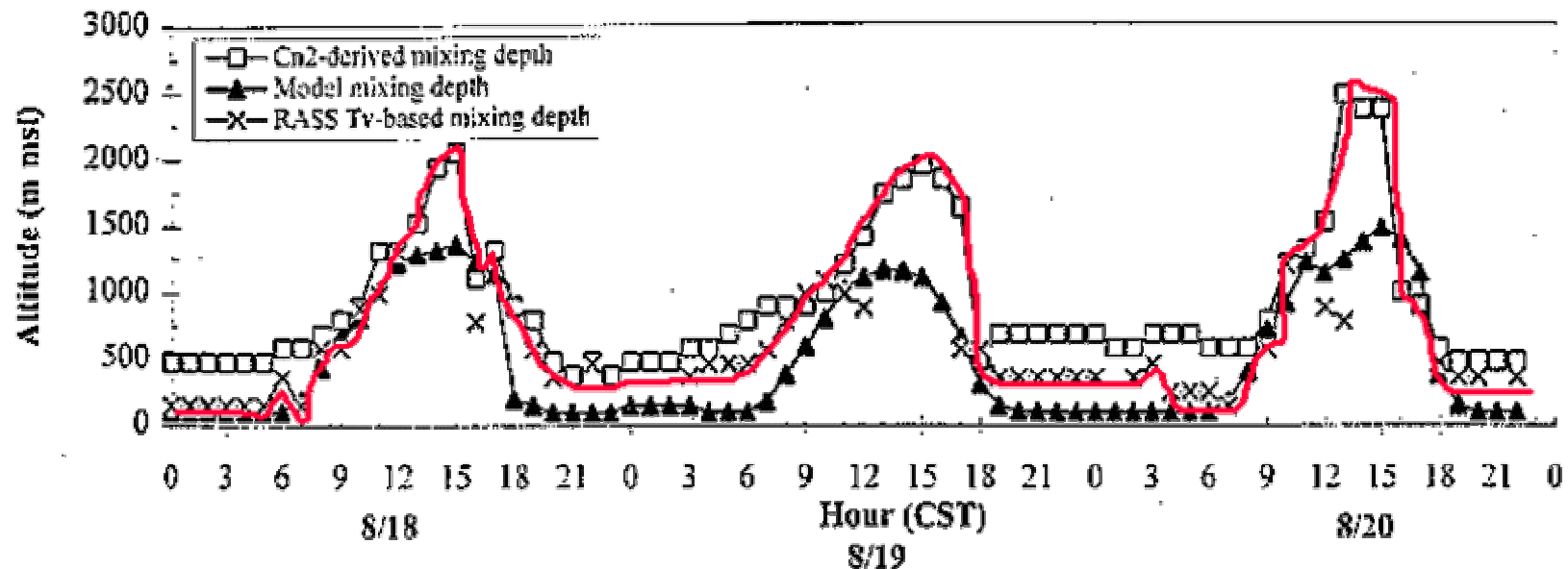
- In addition to comparing to other measurement methods, it is also important to compare C_n^2 -derived mixing depth with model output. In this example, a time series plot of mixing depths estimated from C_n^2 and virtual temperature (T_v) data and from a meteorological model for a radar profiler site in Houston, TX is shown for August 18-20, 1993 (Dye et al., 1995a). During growth and at midday, radar profiler data yield the best estimate of mixing depth. RASS data are superior when mixing heights are low, below 500 m. The bold solid line reflects this best estimate of the mixing height using C_n^2 and T_v.

- The agreement between the model, RASS T_v, and C_n^2 -derived mixing depths is quite good during the growth of the convective boundary layer (CBL - i.e., between 0800 and 1200 CDT). During the later afternoon and at night, discrepancies among all three estimates occurred.

Investigating Boundary Layer Structure and Evolution (1 of 3)

Upper-air meteorological data are useful in assessing boundary layer features including:
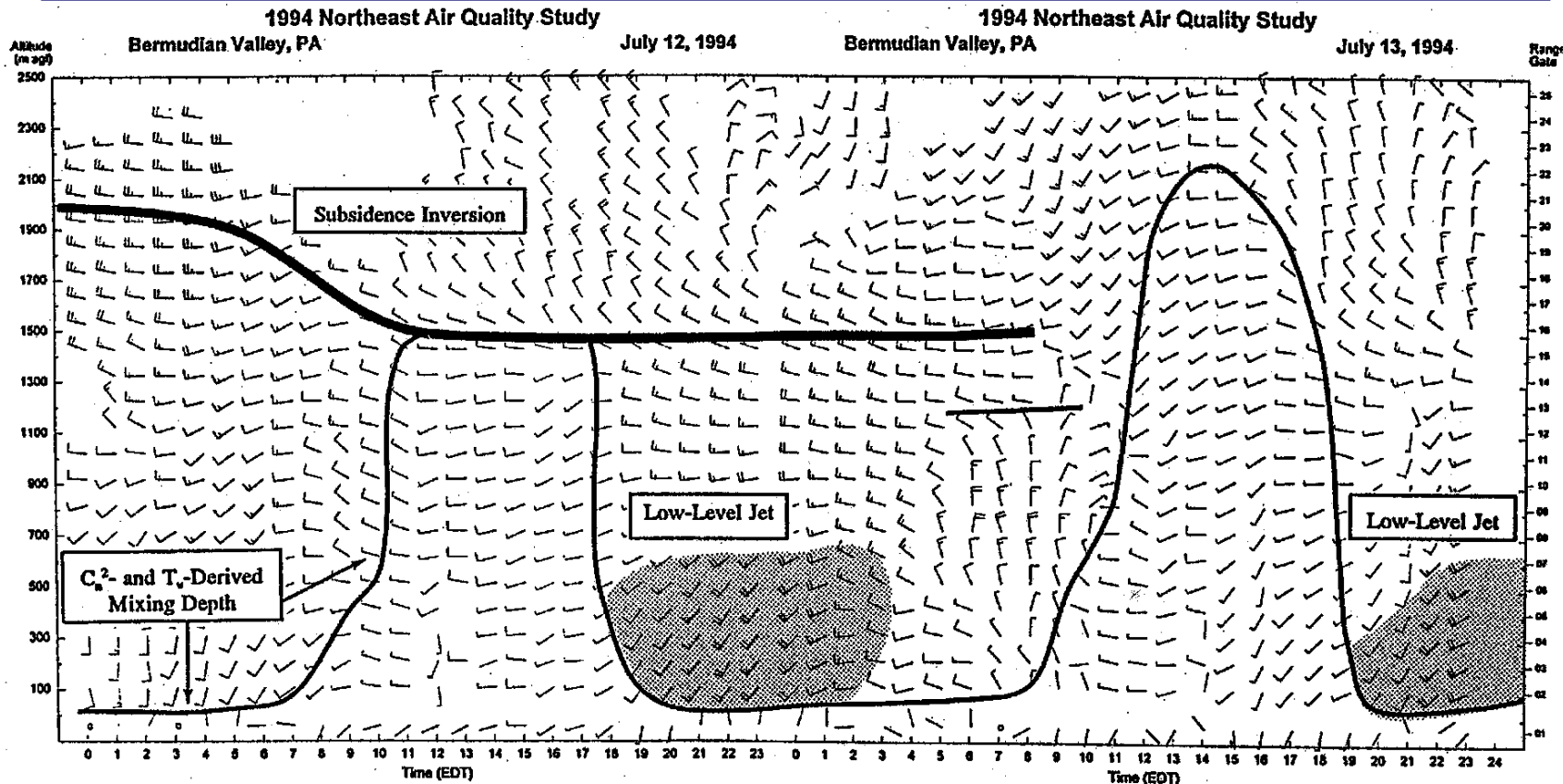
- Nocturnal boundary layer – the boundary layer from sunset to sunrise. It is often characterized by a stable layer, which forms when the solar heating ends and the radiative cooling and surface friction stabilize the lowest part of the atmosphere.

- Evolution of the convective boundary layer – the daytime boundary layer.

- Mixing – The production of turbulent eddies during the daytime is dominated (under clear skies) by heating of the ground surface and (under overcast conditions) by frictional drag. Daytime vertical mixing processes can be vigorous and can produce a well-mixed or nearly uniform vertical concentration profile of an inert tracer.

- Low-level nocturnal jet – a thin stream of fast-moving air (maximum speeds of 10-20 m/s) located 100 to 300 m agl. Nocturnal jets have been observed in many parts of the world and are associated with weather fronts, sloping terrain, ducting and confluence in complex terrain, and inertial oscillation associated with nighttime temperature inversions.

Investigating Boundary Layer Structure and Evolution

Example analyses include:

- Investigate typical profiler/RASS data during episodes; if a nocturnal jet is observed, investigate its frequency and spatial occurrence.

- If non-PAMS upper-air meteorological and air quality data are available (e.g., tethersonde and ozonesonde data), compare measurements and investigate overnight pollutant and meteorological characteristics.

1994 Northeast Air Quality Study — Bermudian Valley, PA — July 12, 1994

1994 Northeast Air Quality Study — Bermudian Valley, PA — July 13, 1994

- This example of upper-air data reveals a recurrent low-level, nocturnal jet. This plot shows a time series cross section of winds, mixing depth, and inversion conditions measured by the radar profiler on July 12-13, 1994 at Bermudian Valley, PA. The thin solid line denotes the height of the mixed layer estimated using C_n^2 and RASS temperature data. The thick line denotes the subsidence inversion.

- The shaded area indicates the region of the nocturnal low-level wind maxima. The maximum mixing depth was significantly different on the two days (Lindsey et al., 1995b).

Isentropic Analysis

- Isentropic analysis refers to locating surfaces of constant potential temperature and examining their structure, their relationships to other meteorological features present in the domain, and the implications of the relationships.

- Constant potential temperature surfaces (called isentropes) can be computed from upper-air temperature, relative humidity, and pressure data. Air parcels flow along isentropes because potential temperature is conserved during adiabatic motion.

- Isentropic cross sections can be used to diagnose the evolution of the boundary layer structure and winds in an evaluation of pollutant transport.

Example Isentropic Analysis

- Upper-air data can help elucidate complex structural features of the atmosphere that directly affect air quality and pollutant transport.

- This example isentropic analysis shows a west-to-east isentropic cross section from Rockford, IL (ROC) to Muskegon, MI (MUS) on June 26, 1991 at 0600 and 1200 CDT. Isentropes are contoured every 2 K. Aloft winds are plotted every 500 m at each rawinsonde site.

- The early morning conditions were characterized by a stable nocturnal boundary layer over land and a stable conduction layer over Lake Michigan. The isentropes show that during the morning, the land breeze and the general offshore flow in Chicago, Gary, and Milwaukee would transport emissions offshore into the conduction layer. Hydrocarbon concentrations measured between 0700-0900 CDT in Chicago and offshore confirmed this type of transport.

- In the afternoon, transport is up and over the lake as illustrated by the isentrope at 302 K.

Dye et al., 1995b
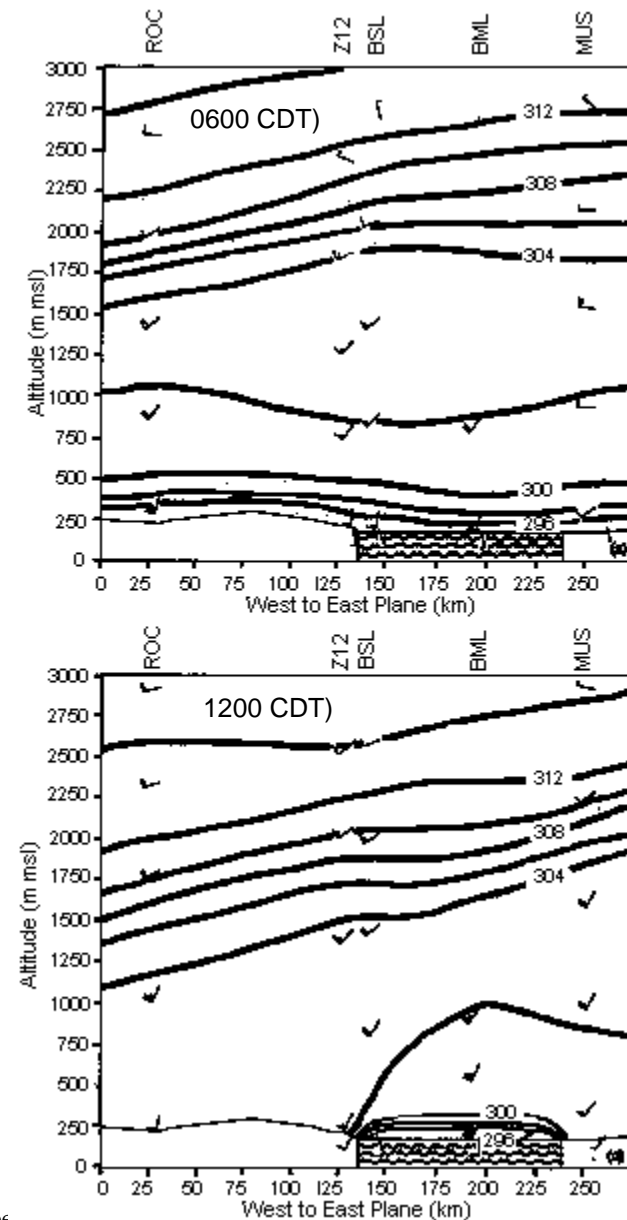
Analysis Objectives

- Diagnose important surface and aloft transport pathways and examine and evaluate key source-receptor relationships in a region.

- Evaluate the potential for long-range transport overnight, and estimate the contribution of aloft carryover of ozone and precursors to regional background concentrations.

- Characterize periods when surface and aloft transport are coupled (i.e., from the same direction), typically during the daytime in the convective boundary layer, versus periods when aloft transport is decoupled from near-surface processes (such as occurs at night as the stable NBL develops).

- Examine the relative roles of same-day transport versus multi-day transport of ozone and precursors to key receptors where exceedances were observed.

- Help develop recommendations for future aloft meteorological and air quality measurement strategies in the region.
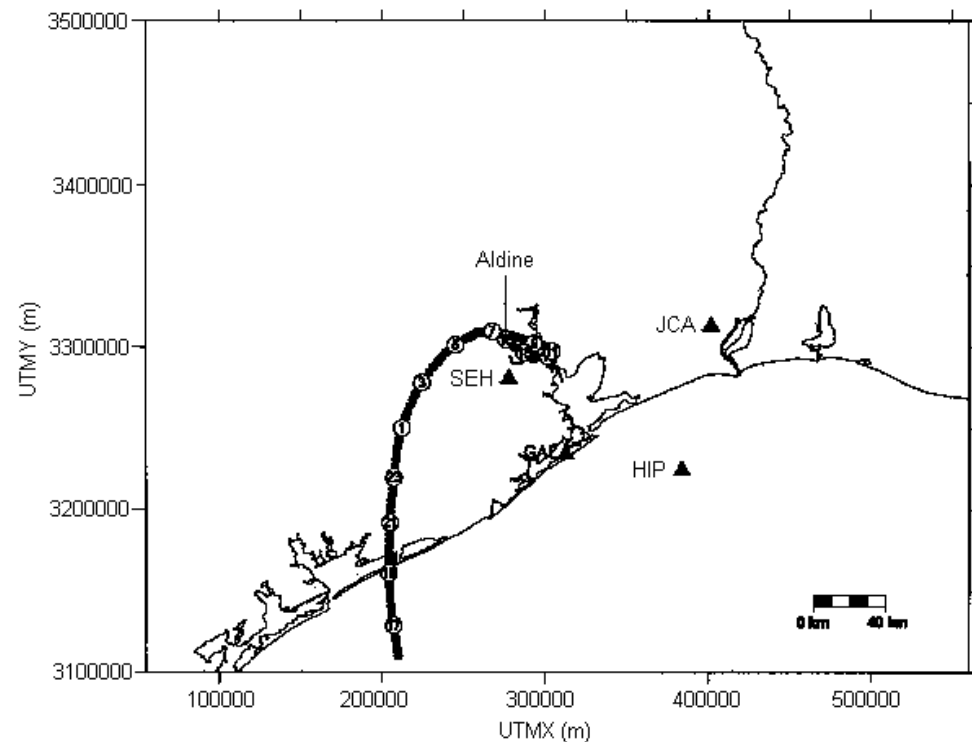
Trajectory Analyses (2 of 2)

Air parcel trajectories estimate the path of a hypothetical air parcel over a selected time period. Upper-air meteorological data are particularly useful since trajectories based on surface meteorological data alone may not be representative of actual transport distances. To perform trajectory analyses:

- Assemble the required data including hourly surface and upper-air wind speed and wind direction.

- Determine physical barriers to airflow.

- Prepare 3-D wind fields for selected periods using the selected wind field model and run a 3-D trajectory model.

- Or, compute wind vectors based on measurements.

- Assess results with respect to other analyses and data.

- This figure shows a trajectory for a parcel of air observed at an altitude of 300 meters. Each symbol represents position in 2-hr increments. The trajectory indicates an eddy, with very little transport occurring from 7:00 a.m. to 4:00 p.m.

- Therefore, during the daytime hours ozone precursors were forming ozone as the air parcel stayed near Aldine.

300-m backward trajectory starting from Aldine, Texas at 1600 CST on August 19, 1993 (SAI et al., 1995).

- Trajectory analyses performed from different sites help build consensus about transport phenomena.

- This example shows four trajectories for air parcels observed at an altitude of 100 meters. Each symbol represents position in 2-hr increments.

- The trajectories indicate that the flow reversal was observed at several sites.
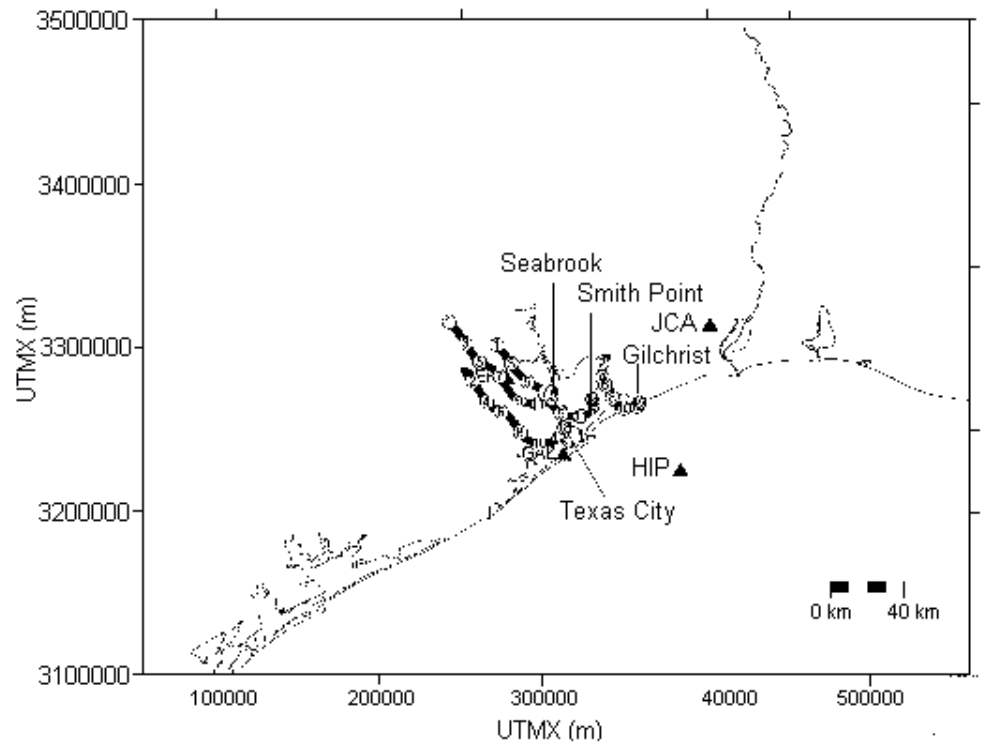
100-m backward trajectories starting from Gilchrist, TX at 1300 CST, Texas City at 1300 CST, Seabrook at 1400 CST, and Smith Point at 1400 CST, on September 8, 1993 (SAI et al., 1995).

- Trajectories should be launched for several hours and from different locations to arrive at a consensus regarding air parcel origins.

- In this example, trajectories were prepared for all hours on a selected day from one location. The trajectories show consistent results including offshore/onshore flow reversal.
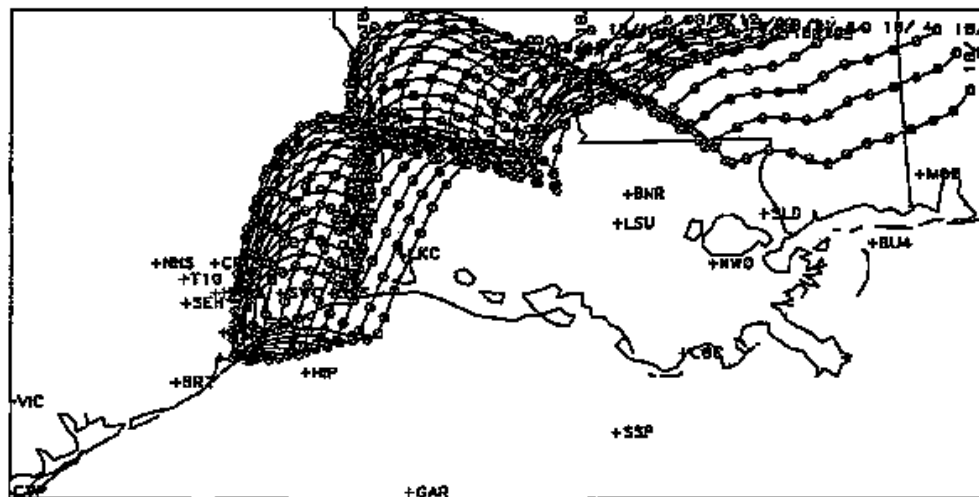
300-m forward trajectories from Galveston, Texas at all hours on August 18 (SAI et al., 1995).

Ventilation and Recirculation Analysis (1 of 2)

- Ventilation (i.e., flow-through) and recirculation analyses are used to investigate transport conditions aloft.

- The procedure discussed here is based on integral quantities computed from profiler data following the work of Allwine and Whiteman (1994).

- Parameters are typically calculated using 12 or 24 hrs of hourly wind data.

- Parameters include:

  S   Scalar wind run (km)

  L   Resultant (vector) transport distance (km)

  Θ Resultant wind directions in degrees from true N adjusted to the proper quadrant

  R   Recirculation factor (*L/S*)

- Recirculation Factor:

  $R = 1$ Straight-line, steady transport occurred during integration period

  $R = 0$ No net transport

  $R \approx 1$ Good ventilation conditions (for L = few hundred km)

  $R < {\sim}0.3$ Recirculation

Example Recirculation Analysis

- This example shows vector integrated transport distances (top), resultant wind directions (middle), and recirculation factors (R) (bottom) calculated from data collected by the southeast Houston (SHE) radar profiler for the period 0600-1700 CDT on August 16, 1993.

- The transport distances in the first few hundred meters were about 175 km with the recirculation factor indicating good ventilation conditions.

- On this day, low ozone concentrations were observed and the aloft winds showed little recirculation.

SAI et al., 1995
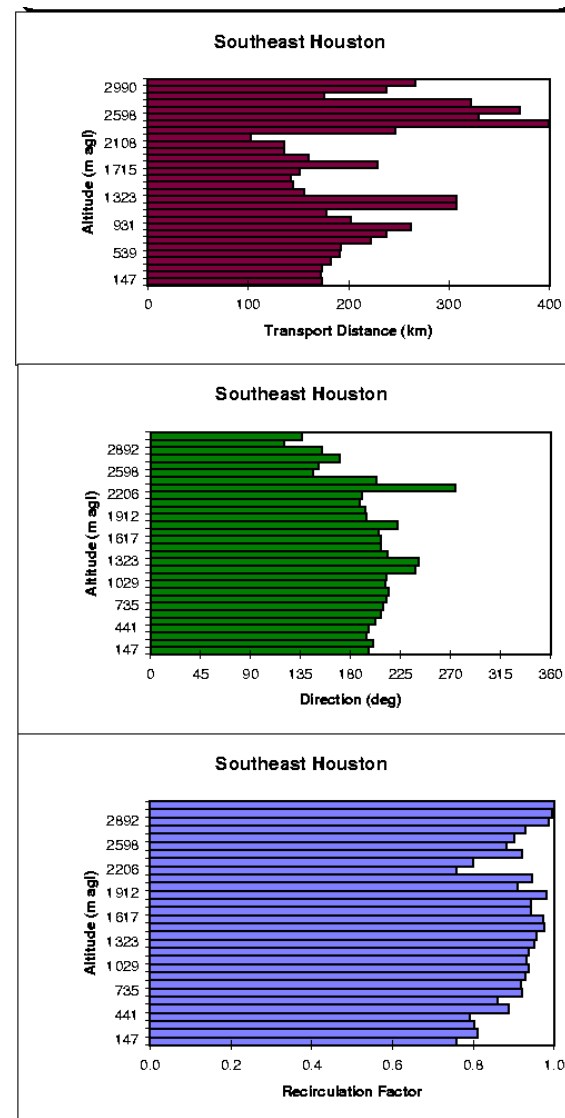
Available Methods and Tools (1 of 2)

PAMS and Non-PAMS Upper-Air Data:

- NOAA profiler network (*http://oak.fsl.noaa.gov/index.html*)

- Special studies such as NARSTO studies in the Northeast, Texas, and California (*http://narsto.owt.com/Narsto/*); Southern Oxidant Study (*http://www.epa.gov/amdweb95/sosda.html*)

- Ozone Lidar (*e.g., http://www2.etl.noaa.gov/uv_dial.html#param*)

Trajectory Methods:

- HYSPLIT (*http://www.arl.noaa.gov/ready.html*)

Surface air quality and meteorological data:

- AIRS Data via public web at *http://www.epa.gov/airsdata*

- AIRS Air Quality System (AQS) via registered users register with EPA/NCC (703-487-4630)

- Meteorological parameters from National Weather Service (NWS) at *http://www.nws.noaa.gov*

- Meteorological parameters from PAMS/AIRS AQS register with EPA/NCC (703-487-4630)

- Private meteorological agencies (e.g., forestry service, agricultural monitoring, industrial facilities)

Summary

- Upper-air wind data are critical to air quality analysis and modeling efforts. The data are used for the assessment of transport characteristics, as direct input to Gaussian dispersion models, and in the initialization and application of meteorological models.

- Upper-air temperature data are used widely in air quality analysis and modeling, including the application and evaluation of meteorological models, and as direct input to air quality models. The vertical temperature structure (stability) influences plume rise and expansion and thus the vertical exchange of pollutants. Temperature also affects photolysis and chemical reaction rates.

- Upper-air data can be used to estimate mixing heights which are important in understanding diurnal variations in pollutant concentrations and pollutant transport.

Allwine K.J. and Whiteman C.D. (1994) Single-station integral measures of atmospheric stagnation, recirculation, and ventilation. *Atmos. Environ*. **28**, 713-721.

Blumenthal D.L., Lurmann F.W., Roberts P.T., Main H.H., MacDonald C.P., Knuth W.R., and Niccum E.M. (1997) Three-dimensional distribution and transport analyses for SJVAQS/AUSPEX. Draft report prepared for the San Joaquin Valleywide Air Pollution Study Agency, California Air Resources Board, Sacramento, CA by Sonoma Technology, Inc., Santa Rosa, CA, STI-91060-1705-DFR, February.

Chang J.C. and Hanna S.R. (1993) Trajectory calculation for selected LMOS periods. Report prepared for Sonoma Technology, Inc., Santa Rosa, CA by Sigma Research Corp., Concord, MA, Report No. 1197-600, May.

Dye T.S. (1996) Unpublished data. Sonoma Technology Inc., Santa Rosa, CA.

Dye T.S., Lindsey C.G., and Anderson J.A. (1995a) Estimates of mixing depths from "boundary layer" profilers. In Preprints of the *9th Symposium on Meteorological Observations and Instrumentation, Charlotte, NC, March 27-31* (STI-94212-1451).

Dye T.S., Roberts P.T., and Korc M.E. (1995b) Observations of transport processes for ozone and ozone precursors during the 1991 Lake Michigan Ozone Study. *J. Appl. Meteorol*. **34**, 1877-1889 (STI-1384).

Gauthreaux Jr. S.A. (1991) The flight behavior of migrating birds in changing wind fields: radar and visual analyses. *Amer. Zool*. **31**, 187-204.

Hanna S.R. and Chang J.C. (1993) Representativeness of 1991 LMOS ozone episodes and relations between ozone episodes and meteorological variables in the Lake Michigan area. Report prepared for Sonoma Technology, Inc., Santa Rosa, CA by Sigma Research Corp., Concord, MA, Report No. 1197-407/411, January.

Lindsey C.G., Dye T.S., Blumenthal D.L., Ray S.E., and Arthur M. (1995a) Meteorological aspects of summertime ozone episodes in the Northeast. Paper FA 5.8 presented at the *9th Joint Conference on the Applications of Air Pollution Meteorology at the 76th AMS Annual Meeting, Atlanta, GA, January 28-February 2, 1996* (STI-1549).

Lindsey C.G., Dye T.S., Roberts P.T., Anderson J.A., and Ray S.E. (1995b) Meteorological aspects of ozone episodes in southeast Texas. Paper No. 95-WP96.02 presented at the *88th Air & Waste Management Association Annual Meeting, San Antonio, TX, June 18-23*.

Main H.H., Chinkin L.R., Haste T.L., Roberts P.T., and Reiss R. (1997) Shasta County ozone and ozone precursor transport quantification study. Final report prepared for the Shasta County Department of Resource Management, Redding, CA, STI-95180-1714-FR, March.

Roberts P.T. and Main H.H. (1992) Characterization of three-dimensional air quality during the SCAQS. In Southern California Air Quality Study Data Analysis. Proceedings from *SCAQS Data Analysis Conference, University of California, Los Angeles, CA, July 21-23*, Air & Waste Management Association, Pittsburgh, PA (STI-1223).

Roberts P.T., Main H.H., Smith T.B., Lindsey C.G., and Korc M.E. (1992a) Analysis of 3-D air quality data and carbon, nitrogen, and sulfur species distributions during the Southern California Air Quality Study. Final report prepared for the Coordinating Research Council, Atlanta, GA by Sonoma Technology, Inc., Santa Rosa, CA, STI-99100-1213-FR, October.

Roberts P.T., Musarra S., Smith T.B., and Lurmann F.W. (1992c) A study to determine the nature and extent of ozone and ozone precursor transport in selected areas of California. Final report prepared for the California Air Resources Board, Sacramento, CA by Sonoma Technology, Inc., Santa Rosa, CA, STI-90060-1162-FR, December.

Roberts P.T., Main H.H., Lindsey C.G., and Korc M.E. (1993a) Ozone and particulate matter case study analysis for the Southern California Air Quality Study. Final report prepared for the California Air Resources Board, Sacramento, CA by Sonoma Technology, Inc., Santa Rosa, CA, STI-90020-1222-FR, May.

Roberts P.T., Main H.H., and Korc M.E. (1993b) Comparison of 3-D air quality data with model sensitivity runs for the South Coast Air Basin. Paper No. 93-WP-69B.05 presented at the *Air & Waste Management Association Regional Photochemical Measurement and Modeling Studies Conference, San Diego, CA, November 8-12* (STI-1244).

Roberts P.T., Dye T.S., Korc M.E., and Main H.H. (1994) Air quality data analysis for the 1991 Lake Michigan Ozone Study. Final report prepared for Lake Michigan Air Directors Consortium, Des Plaines, IL by Sonoma Technology, Inc., Santa Rosa, CA, STI-92022-1410-FR.

Roberts P., Korc M., Blumenthal D., and Mueller P.K. (1995a) NARSTO-Northeast 1995 summer ozone study. Version 1. Report prepared for Electric Power Research Institute, Palo Alto, CA by Sonoma Technology, Inc., Santa Rosa, CA, STI-95135-1538-WD1; Research project EPRI WO9108-01.

Systems Applications International, Sonoma Technology Inc., Earth Tech, and Alpine Geophysics (1995) Gulf of Mexico Air Quality Study. Vol 1: Summary of data analysis and modeling. Draft final report prepared for U.S. Department of the Interior, Minerals Management Service, Gulf of Mexico OCS Region, New Orleans, LA, OCS Study, MMS 94-0046, SYSAPP-95/013d.

Tremback C.J. and Lyons W.A. (1993) Trajectory calculation derived from CALRAMS simulations. Report prepared for Lake Michigan Air Directors Consortium, Des Plaines, IL by ASTeR, Inc., Ft. Collins, CO, August.

U.S. Environmental Protection Agency (1995) Draft guidelines for the quality assurance and management of PAMS upper-air meteorological data.

U.S. Environmental Protection Agency (2000) Meteorological monitoring guidance for regulatory modeling applications. Office of Air Quality Planning and Standards, Research Triangle Park, NC, EPA-454/R-99-005, February.

White A.B. (1993) Mixing depth detection using 915 MHz radar reflectivity data. In *Preprints, AMS 8th Symposium on Meteorological Observations and Instruments, Anaheim, CA, January 17-22*.

Wilczak J.M., Strauch R.G., Weber B.L., Merritt D.A., Ralph F.M., Jordan J.R., Wolfe D.E., Lewis L.K., Wuertz D.B., Gaynor J.E., McLaughlin S., Rogers R., Riddle A., and Dye T. (1995) Contamination of wind profiler data by migrating birds: characteristics of corrupted data and potential solutions. *J. of Oceanic and Atmos. Tech.*, **12**, 449-467.

Wyngaard J.C. and LeMone M.A. (1980) Behavior of the refractive index structure parameter in the entraining convective boundary layer. *J. Atmos. Sci.*, **37**, 1573-1585.